THE STRUCTURE AND COMPOSITION OF URANOSPATHITE, $Al_{1-x}\square_x[(UO_2)(PO_4)]_2(H_2O)_{20+3x}F_{1-3x}$, $0 < x < 0.33$, A NON-CENTROSYMMETRIC FLUORINE-BEARING MINERAL OF THE AUTUNITE GROUP, AND OF A RELATED SYNTHETIC LOWER HYDRATE, $Al_{0.67}\square_{0.33}[(UO_2)(PO_4)]_2(H_2O)_{15.5}$

ANDREW J. LOCOCK[§]

Mineralogy, Department of Natural History, Royal Ontario Museum, 100 Queen's Park, Toronto, Ontario M5S 2C6, Canada

WILLIAM S. KINMAN AND PETER C. BURNS

Department of Civil Engineering and Geological Sciences, University of Notre Dame,
156 Fitzpatrick Hall, Notre Dame, Indiana 46556, U.S.A.

ABSTRACT

The crystal structure of uranospathite, ideal formula $Al_{1-x}\square_x[(UO_2)(PO_4)]_2(H_2O)_{20+3x}F_{1-3x}$, $0 < x < 0.33$, orthorhombic, space group $Pnn2$, a 30.020(4), b 7.0084(9), c 7.0492(9) Å, V 1483.1(3) Å^3, $Z = 2$, D_{calc} 2.54 g/mL, and that of synthetic $Al_{0.67}\square_{0.33}$ $[(UO_2)(PO_4)]_2(H_2O)_{15.5}$, *AlUP*, triclinic, space group $P\bar{1}$, a 7.0020(6), b 13.7120(11), c 14.0243(11) Å, α 78.418(2), β 89.676(2), γ 81.863(2)°, V 1305.4(2) Å^3, $Z = 2$, D_{calc} 2.61 g/mL, were refined by full-matrix least-squares techniques on the basis of F^2 to agreement indices $R1$ (uranospathite and *AlUP*) of 4.0 and 4.9%, calculated for 2980 and 4545 unique observed reflections ($|F_o| \geq 4\sigma_F$), and wR_2 of 9.0 and 14.1% for all data, respectively. Intensity data were collected at room temperature using Mo$K\alpha$ radiation and a CCD-based area detector. Uranospathite and *AlUP* contain the autunite-type sheet with composition $[(UO_2)(PO_4)]^-$, which involves the sharing of equatorial vertices of uranyl square bipyramids with phosphate tetrahedra. In both uranospathite and *AlUP*, aluminum occurs as isolated $Al(H_2O)_6$ octahedra, which are held in the interlayer by a complex network of H-bonding involving an additional eight and ten symmetrically independent H_2O groups, respectively, some of which form square-planar sets both above and below the Al octahedra. The arrangement of the interlayer H_2O groups in uranospathite leads to tilting of the Al octahedra, and prevents the structure from being centrosymmetric. The presence of F in both uranospathite and its As analogue, arsenuranospathite, was confirmed by qualitative wavelength-dispersion X-ray emission spectroscopy and appears to be necessary to maintain electroneutrality in the crystals studied. Charge balance is maintained in the synthetic aluminum uranyl phosphate hydrate *AlUP* by partial occupancy of the Al position.

Keywords: uranospathite, arsenuranospathite, autunite, uranyl phosphate, uranyl arsenate, fluorine, crystal structure.

SOMMAIRE

Nous avons établi la structure cristalline de l'uranospathite, de formule idéale $Al_{1-x}\square_x[(UO_2)(PO_4)]_2(H_2O)_{20+3x}F_{1-3x}$, $0 < x <$ 0.33, orthorhombique, groupe spatial $Pnn2$, a 30.020(4), b 7.0084(9), c 7.0492(9) Å, $Z = 2$, D_{calc} 2.54 g/mL, et celle du composé synthétique $Al_{0.67}\square_{0.33}[(UO_2)(PO_4)]_2(H_2O)_{15.5}$, *AlUP*, triclinique, groupe spatial $P\bar{1}$, a 7.0020(6), b 13.7120(11), c 14.0243(11) Å, α 78.418(2), β 89.676(2), γ 81.863(2)°, V 1305.4(2) Å^3, $Z = 2$, D_{calc} 2.61 g/mL, par techniques de moindres carrés à matrice entière en utilisant les facteurs F^2 jusqu'à un résidu $R1$ (uranospathite et *AlUP*) de 4.0 et 4.9%, calculé pour 2980 et 4545 réflexions uniques observées ($|F_o| \geq 4\sigma_F$), et un wR_2 de 9.0 et de 14.1% calculé en utilisant toutes les données, respectivement. Les intensités ont été mesurées à température ambiante en utilisant un rayonnement Mo$K\alpha$ et un détecteur à aire de type CCD. L'uranospathite et le *AlUP* contiennent un feuillet de type autunite, de composition $[(UO_2)(PO_4)]^-$, qui implique un partage des coins équatoriaux des bipyramides carrées à uranyle avec des tétraèdres de phosphate. Dans l'uranospathite et le *AlUP*, l'aluminium se trouve dans des octaèdres $Al(H_2O)_6$ isolés, retenus dans l'interfeuillet grâce à un réseau complexe de liaisons hydrogène impliquant de huit à dix groupes H_2O symétriquement indépendants, respectivement, dont certains forment des agencements carrés par dessus et par dessous les octaèdres à Al. L'arrangement des groupes H_2O dans l'interfeuillet de l'uranospathite mène à une inclinaison des octaèdres à Al, et empêche la structure d'être centrosymétrique. La présence de F dans l'uranospathite et son analogue à dominance en As, l'arsenuranospathite, a été confirmée par spectroscopie

§ *E-mail address*: andrewl@rom.on.ca

des rayons X émis en dispersion de longueurs d'ondes, et semble nécessaire pour assurer l'électroneutralité des cristaux étudiés. L'électroneutralité dans le phosphate uranylé d'aluminium hydraté synthétique *AlUP* est assuré par l'occupation partielle du site Al.

<div align="right">(Traduit par la Rédaction)</div>

Mots-clés: uranospathite, arsenuranospathite, autunite, phosphate à uranyle, arsenate à uranyle, fluor, structure cristalline.

Introduction

Uranyl phosphates and uranyl arsenates are amongst the most abundant, widespread and least soluble of uranium minerals, constituting more than a third of the ~200 described uranium minerals (Finch & Murakami 1999). In natural systems, only a few trivalent metals [Al^{3+}, Bi^{3+}, Fe^{3+} and Nd^{3+}] are incorporated into the structures of uranyl phosphates and uranyl arsenates; the aluminum-bearing minerals are not only the most common, but form the largest number of species (Mandarino & Back 2004).

At least twelve aluminum uranyl phosphate minerals have been described, of which only sabugalite, $(HAl)_{0.5}[(UO_2)(PO_4)]_2(H_2O)_{8-10}$, threadgoldite, $Al[(UO_2)(PO_4)]_2(OH)(H_2O)_8$, and uranospathite, $(HAl)_{0.5}[(UO_2)(PO_4)]_2(H_2O)_{20}$, contain the autunite-type sheet (Walenta 1978, Khosrawan-Sazedj 1982, Vochten & Pelsmaekers 1983); only threadgoldite has a previously determined structure. Althupite, $AlTh(UO_2)[(UO_2)_3O(OH)(PO_4)_2]_2(OH)_3(H_2O)_{15}$, mundite, $Al[(UO_2)_3(PO_4)_2(OH)_2](OH)(H_2O)_{5.5}$, phuralumite, $Al_2[(UO_2)_3(OH)_2(PO_4)_2](OH)_4(H_2O)_{10}$, and upalite, $Al[(UO_2)_3O(OH)(PO_4)_2](H_2O)_7$, belong to the phosphuranylite group (Piret & Deliens 1987, Deliens & Piret 1981, Piret *et al.* 1979b, Piret & Declercq 1983); of these, only the structure of mundite has not been refined. The minerals furongite, $Al_2(UO_2)_2(PO_4)_3(OH)(H_2O)_{13.5}$, kamitugaite, $PbAl(UO_2)_5[(P,As)O_4]_2(OH)_9(H_2O)_{9.5}$, moreauite, $Al_3(UO_2)(PO_4)_3(OH)_2(H_2O)_{13}$, ranunculite, $Al(H_3O)(UO_2)(PO_4)(OH)_3(H_2O)_3$, and triangulite, $Al_3(UO_2)_4(PO_4)_4(OH)_5(H_2O)_5$, are currently of undetermined structural affinity (Deliens & Piret 1979b, 1982, 1984, 1985a, b). As part of our ongoing research on the structures of uranyl phosphates and uranyl arsenates, we have determined the crystal structures of uranospathite, a highly hydrated aluminum uranyl phosphate of the autunite group, and a related synthetic lower hydrate, $Al_{0.67}\square_{0.33}[(UO_2)(PO_4)]_2(H_2O)_{15.5}$, *AlUP*.

Previous Studies

Uranospathite was originally described by Hallimond (1915) as a member of the autunite group; it was discovered in material from the Redruth mining area of Cornwall, United Kingdom (Embrey & Symes 1987). Uranospathite was reported to have orthorhombic (pseudotetragonal) symmetry, density 2.50 g/mL, biaxial negative optics, and pale to deep yellow pleochroism. No chemical data were presented, but its absorption spectrum was stated to be consistent with a uranyl compound and its behavior in a desiccator indicated that it is hydrated (Hallimond 1915).

Frondel (1954, 1958) questioned the identity of uranospathite based on examinations of type and non-type material, and concluded that it is a more highly hydrated member of the torbernite–zeunerite series: $Cu[(UO_2)(PO_4)]_2(H_2O)_{12}$ – $Cu[(UO_2)(AsO_4)]_2(H_2O)_{12}$. Hallimond (1954) agreed that uranospathite is a higher hydrate than torbernite or zeunerite, but because of the yellow color of the material, disputed the presence of significant copper.

Walenta (1978) re-investigated uranospathite from the type locality and showed that it is a highly hydrated aluminum uranyl phosphate of the autunite group, with the chemical formula $(HAl)_{0.5}[(UO_2)(PO_4)]_2(H_2O)_{20}$. The material investigated by Frondel was interpreted to have been impure. In the same report, the As analogue of uranospathite was described as the new species arsenuranospathite, $(HAl)_{0.5}[(UO_2)(AsO_4)]_2(H_2O)_{20}$ (Walenta 1978), on the basis of material from Menzenschwand, Germany. Although the tetragonal space-group $P4_2/n$ was suggested by Walenta (1978) for both minerals, their optical characters are biaxial negative, consistent only with lower symmetry. Uranospathite and arsenuranospathite were reported to be unstable under normal conditions, with several lower hydration states described (16, 10, and 8 H_2O groups per formula unit); both the decahydrate, and more usually the octahydrate, have been considered identical with sabugalite (Frondel 1951, Walenta 1965, 1978, Vochten & Pelsmaekers 1983, Čejka 1999, Finch & Murakami 1999, Anthony *et al.* 2000).

Uranospathite and arsenuranospathite are rare but widely distributed species, with occurrences known in the United Kingdom (Hallimond 1915, Embrey & Symes 1987), France (Chervet & Branche 1955, Deliens *et al.* 1991), Germany (Walenta 1978, Bültemann 1979), Macedonia (Saric 1978), Spain and Australia (Anthony *et al.* 2000). Further information on localities is listed at www.mindat.org.

EXPERIMENTAL

The uranospathite and arsenuranospathite specimens studied are from the collections of the Institut Royal des Sciences Naturelles de Belgique (the Royal Belgian Institute of Natural Sciences) in Brussels: samples RC3982, RC4374 and RC4154, and from the Mineralogical and Geological Museum of Harvard University: samples 98068 and uncatalogued 17–F and 15C (Table 1). Owing to the paucity of material, only sample 15C was investigated by powder X-ray diffraction (using a Bruker D8 diffractometer and Cu$K\alpha$ radiation). This sample was ground in alumina under water and mounted on an offcut single-crystal Si wafer; the powder pattern exhibited severe preferred orientation and yielded a basal spacing of 9.2 Å, and is interpreted (in conjunction with qualitative EDS data) to be consistent with a lower hydrate of phosphatian aluminum uranyl arsenate. Attempts to rehydrate powdered material from sample 15C using ultrapure water were not successful.

Crystals of $Al_{0.67}\square_{0.33}[(UO_2)(PO_4)]_2(H_2O)_{15.5}$, *AlUP* were grown at room temperature over four months by slow diffusion of 0.1 M H_3PO_4 $_{(aq)}$ and 0.1 M $UO_2(NO_3)(H_2O)_6$ $_{(aq)}$ into Al-bearing silica gel. The gel was formed by the hydrolysis of a mixture (1:10) of $(CH_3O)_4Si$ $_{(liq)}$ and 0.10 M $AlCl_3(H_2O)_6$ $_{(aq)}$ (method modified after Arend & Connelly 1982, Manghi & Polla 1983, Zolensky 1983, Perrino & LeMaster 1984, Robert & LeFaucheux 1988, Henisch 1988).

Electron-microprobe examination

Qualitative electron-microprobe analysis was used to confirm the compositions of the uranospathite and arsenuranospathite samples studied, as the volume of available material permitted powder X-ray diffraction in the case of sample 15C only. Crystals were mounted on adhesive carbon tabs and carbon-coated. Quantitative analysis was not attempted because of the beam-sensitive nature of uranospathite and arsenuranospathite; these minerals dehydrate under the electron beam, leading to considerable beam-induced damage (Fig. 1). Energy-dispersion X-ray emission spectra (EDS) were acquired with an ultra-thin-window Si(Li)

detector on a JEOL JXA–8600 Superprobe with a 5 μm diameter beam at an excitation voltage of 15 kV and probe currents of 1.5–3.0 nA. Optical examination of material from samples 17–F and RC4154 revealed the presence of associated epitactic (meta)torbernite and (meta)zeunerite, respectively, and these were confirmed by EDS results. We detected U, As, P, Al, and O by EDS analysis in uranospathite and arsenuranospathite (Fig. 2).

In conjunction with the results of the single-crystal determination of the structure of uranospathite, the EDS results did not yield an electroneutral formula; an excess positive charge was apparent. In order to test for the presence of F, wavelength-dispersion X-ray emission spectra were acquired in the energy range 0.63–0.77 keV for samples 17–F, 15C, 98068, RC4374 and RC4154. Unfortunately, it did not prove possible to recover the crystal from which the structure was determined, and no further crystals were available from this sample (RC3982) at the time of examination using wavelength-dispersion spectrometry (WDS). WDS analysis was undertaken with an excitation voltage of 15 keV, probe current of 10 nA, spectrometer step-size 0.01 mm (0.07–0.10 eV over the energy range examined), and count times of 0.05 – 1.00 s per step, on unpolished carbon-coated crystals mounted on carbon tabs, and on well-polished carbon-coated standards (Table 2). A W/Si multilayer crystal was used (LDE–1, $2d = 60$ Å) for the scans, as multiple-order interferences higher than second-order are effectively absent in this type of spectrometer (Reed 1993, Raudsepp 1995, Ottolini *et al.* 2000). Examination of the fluorapatite standard confirmed that the third-order interference from P$K\alpha$ was not present. The W/Si crystal was calibrated using

TABLE 1. SAMPLES EXAMINED

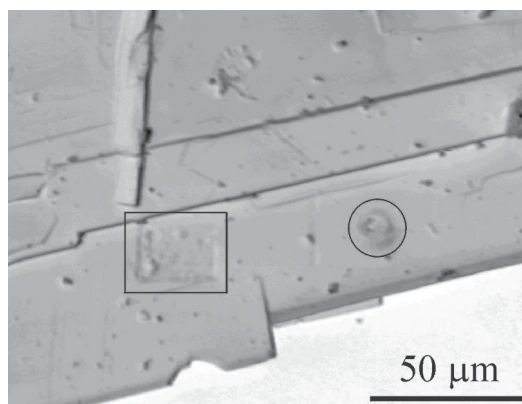| Mineral	Sample #	Locality
uranospathite	RC3982	Vénachat, Haute-Vienne, France
uranospathite	17-F	Redruth area, Cornwall, U.K.
arsenuranospathite	15C	Wheal Basset, near Redruth, Cornwall, U.K.
arsenuranospathite	98068	Wheal Basset, near Redruth, Cornwall, U.K.
arsenuranospathite	RC4374	Krunkelbach deposit, Menzenschwand, Baden-Württemberg, Germany
arsenuranospathite	RC4154	Rabejac, Lodève, Hérault, France

FIG. 1. Secondary electron micrograph of arsenuranospathite, sample RC4374, shown in inverted contrast. The circle and rectangle outline beam damage from a point analysis and from a rastered area, respectively.
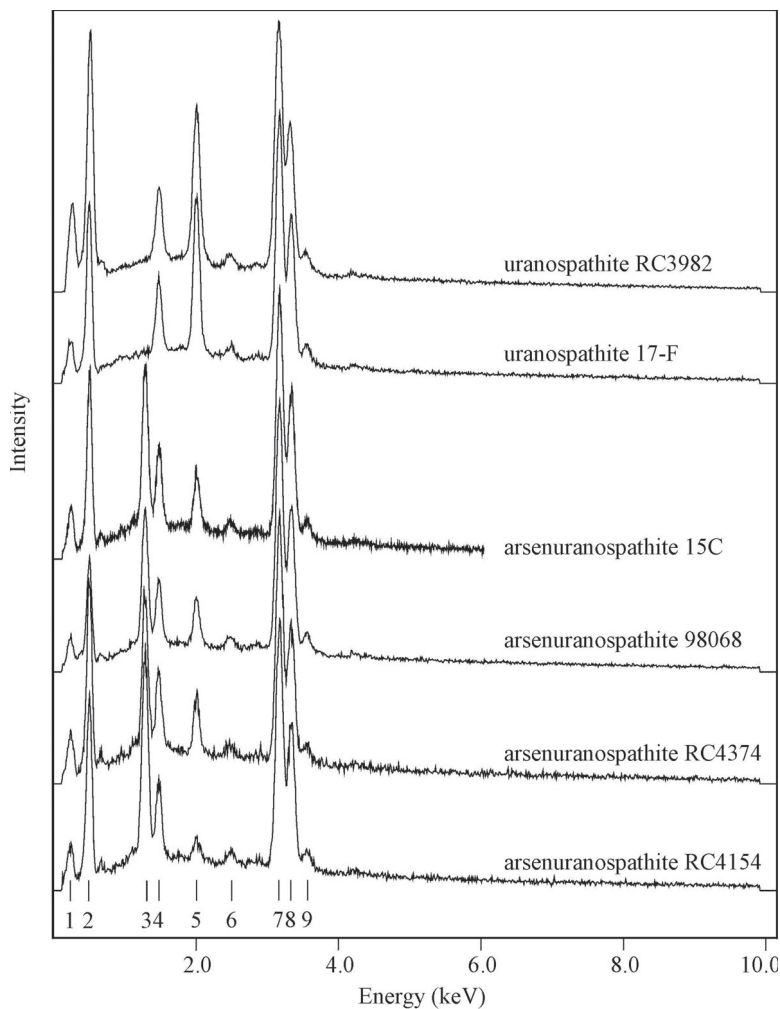
F<small>IG</small>. 2.   Energy-dispersion X-ray emission spectra of uranospathite and arsenuranospa-
thite. The labeled EDS peaks correspond to the following X-ray lines: 1: C$K\alpha$, 2:
O$K\alpha$, 3: overlapped As$L\alpha_1$ and As$L\beta_1$, 4: Al$K\alpha$, 5: P$K\alpha$, 6: U$M\zeta$, 7: U$M\alpha$, 8: U$M\beta$,
and 9: U$M\gamma$.

the second-order emission lines from As and Al; despite
this precaution, the fluorine emission line is shifted to
0.668 keV (from ideal 0.677 keV) in both the standards
(fluorapatite, barium fluoride) and the samples. The
presence of F was confirmed in all five of the urano-
spathite and arsenuranospathite samples analyzed by
qualitative WDS. Figure 3 shows representative WDS
scans for samples RC4154 and 98068, along with
spectra from the standards for comparison.

Single-crystal X-ray diffraction

Of the samples of uranospathite and arsenurano-
spathite studied, only sample RC3982 proved to have
crystals of sufficient quality for structure determination.
Crystals from this sample are highly fluorescent under
illumination by a mixed long-wave and short-wave
UV source. Initially, an optically homogeneous crystal
was coated in two-part epoxy, glued to a glass fiber,
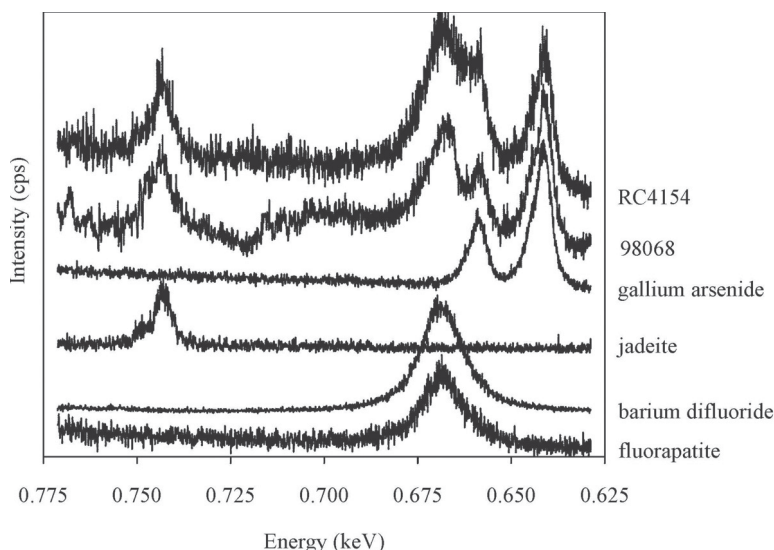and mounted on a Bruker PLATFORM three-circle X-

Fɪɢ. 3. Wavelength-dispersion X-ray emission spectra of arsenuranospathite and standards. The peaks correspond to the following X-ray lines: 0.743 keV: second-order AlKα, 0.668 keV: FKα, 0.659 keV: second-order AsLβ₁, and 0.641 keV: second-order AsLα₁. Spectra have been scaled for ease of comparison. The irregular background for arsenuranospathite 98068 is a result of beam damage accumulating at a single point over the course of the WDS scan. Arsenuranospathite RC4154 exhibits a more regular background; for this sample, the beam was rastered over a 17 × 25 μm area.

ray diffractometer operated at 50 keV and 40 mA and equipped with a 4K APEX CCD detector with a crystal-to-detector distance of 4.7 cm. During the course of data acquisition, the cell dimensions were monitored, and we found that the *a* cell dimension decreased quickly with time, and the mosaic spread increased until the diffraction pattern could no longer be indexed or the sample described as a single crystal. The primary mode of X-ray attenuation in solids is by absorption, and we interpret that the heat generated by the impinging X-ray beam caused the dehydration of the crystal.

Subsequently, another optically homogeneous crystal of uranospathite was captured in a 0.5 mm diameter glass capillary (Charles Supper Co.) with Millepore-filtered ultrapure water (18 MΩ resistance) and immobilized with high-vacuum silicone grease (Dow Corning). A crystal of *AlUP* was mounted separately in the same fashion. The encapsulated crystals were mounted on a Bruker PLATFORM three-circle X-ray diffractometer operated at 50 keV and 40 mA and equipped with a 4K APEX CCD detector with a crystal-to-detector distance of 4.7 cm. A sphere of three-dimensional data was collected at room temperature for both crystals using graphite-monochromatized MoKα X-radiation and frame widths of 0.3° in ω, with count-times per frame of 20 seconds. Details of the data acquisition and refinement parameters are provided in Table 3. The intensity data were reduced and corrected for Lorentz, polarization, and background effects using the program SAINT (Bruker 1998), and the unit-cell dimensions were refined using least-squares techniques. Comparison of the intensities of equivalent reflections measured at different times during data acquisition showed no significant decay for either compound.

Scattering curves for neutral atoms, together with anomalous dispersion corrections, were taken from *International Tables for X-ray Crystallography, Vol. C* (Wilson 1992). The SHELXTL Version 5 series of programs was used for the solution and refinement of the crystal structures (Sheldrick 2000).

Structure solution and refinement

The presence in the primary X-ray beam of amorphous components (glass capillary, water and vacuum grease) gives rise to a background of significant diffuse scattering on the CCD area detector, the intensity of which varies with the changes in geometry of the capillary and crystal relative to the X-ray beam and detector during data collection. This effect was not observed with the unencapsulated crystal. The presence of significant diffuse scattering appears to have contributed some ambiguity to the accurate determination of systematic absences of reflections, and thus to the determination

of the space group of uranospathite. To avoid this difficulty, the structure of uranospathite was solved by Patterson methods and was refined on the basis of F^2 for all unique data in space group $P1$ (no symmetry). All non-H atoms were located and a structure model including anisotropic displacement parameters for U atoms converged, and gave an agreement index ($R1$) of 5.9%, calculated for the observed unique reflections ($|F_o| \geq 4\sigma_F$).

This triclinic solution was tested for higher symmetry with the ADDSYM algorithm in the program PLATON (Le Page 1987, Spek 2003), and transformed to space group $Pnn2$. A structure model in $Pnn2$ including the inversion twin law [$\bar{1}00/0\bar{1}0/00\bar{1}$] and anisotropic displacement parameters for U, P, and Al converged, and gave an agreement index ($R1$) of 4.0%, calculated for the 2980 observed unique reflections ($|F_o| \geq 4\sigma_F$). The inversion-twin-component scale factor refined to 0.46(2), consistent with an even distribution of the enantiomorphic components. The final value of wR_2 was 9.0% for all data using the structure-factor weights assigned during least-squares refinement. The locations of the H atoms in the unit cell were not determined. The

largest correlation-matrix element was not overly high, with a value of 0.855.

Refinement in space groups $Pnnn$, $Pnna$ and $Pnnb$ yielded large numbers of intense violations of the systematic absences. Refinement in the centrosymmetric space-group $Pnnm$ gave physically unrealistic interatomic distances for the phosphate and uranyl polyhedra, and the interlayer contents were highly disordered. This model did not converge, and had an agreement index ($R1$) of 7.6%. The non-centrosymmetric description in space group $Pnn2$ is preferred for the structure of uranospathite, as the correlation-matrix elements are not overly high, all of the atoms are ordered, and the agreement index is considerably lower than in the model with space group $Pnnm$ (cf. Marsh 1995). Uranospathite appears to be one of only a few noncentric compounds that contain the autunite-type sheet.

The lack of systematic absences of reflections for $AlUP$ was consistent with space groups $P1$ and $P\bar{1}$. The structure of $AlUP$ was solved by direct methods and was refined on the basis of F^2 for all unique data in space group $P\bar{1}$. A structure model including anisotropic displacement parameters for U and P converged, and gave an agreement index ($R1$) of 4.9%, calculated for the 4545 observed unique reflections ($|F_o| \geq 4\sigma_F$). The final value of wR_2 is 14.1% for all data using the structure-factor weights assigned during least-squares refinement. The locations of the H atoms in the unit cell were not determined.

The positional parameters of atoms in uranospathite and $AlUP$ are given in Tables 4 and 5, anisotropic displacement parameters are in Tables 6 and 7, and selected interatomic distances are in Tables 8 and 9,

TABLE 3. CRYSTALLOGRAPHIC DATA AND REFINEMENT PARAMETERS

Compound	RC3982 uranospathite	AlUP
a (Å)	30.020(4)	7.0020(6)
b (Å)	7.0084(9)	13.7120(11)
c (Å)	7.0492(9)	14.0243(11)
α, β, γ (°)	90, 90, 90	78.418(2), 89.676(2), 81.863(2)
V (Å³)	1483.1(3)	1305.4(2)
Space group	$Pnn2$	$P\bar{1}$
Z	2	2
Formula	$Al_{0.86}\square_{0.14}[(UO_2)(PO_4)]_2$ $(H_2O)_{20.42}F_{0.58}$	$Al_{0.67}\square_{0.33}[(UO_2)(PO_4)]_2$ $(H_2O)_{15.5}$
Formula weight	1132.09	1027.31
$F(000)$	1061.2	947
μ (mm⁻¹)	11.16	12.64
D_{calc} (g/mL)	2.54	2.61
Crystal size (mm)	$0.16 \times 0.08 \times 0.02$	$0.12 \times 0.12 \times 0.02$
Color and habit	pale yellow plate	pale yellow plate
Temperature (K)	293(2)	293(2)
Frame width (°), time (s)	0.3, 20	0.3, 20
Collection, hours	sphere, 16	sphere, 16
θ range	2.97 – 34.57	1.90 – 34.49
Data collected	$h \pm 47, -10 \leq k \leq 11,$ $-10 \leq l \leq 11$	$h \pm 11, k \pm 21, l \pm 22$
Absorption*	plate (100) 3°	ellipsoid
Total reflections	22404	26882
Unique reflections, R_{int}	6014, 12.3%	10628, 10.8%
Unique $|F_o| \geq 4\sigma_F$	2980	4545
Parameters	92	148
$R1$† for $|F_o| \geq 4\sigma_F$‡	4.0%	4.9%
$R1$† all data, wR_2‡	9.7, 9.0%	12.7, 14.1%
Weighting a	0.0156	0.039
Goodness of fit	0.836	0.961
Mean shift/esd	0.000	0.000
Peaks (e/Å³)	1.9, −1.7	3.8, −2.5

* Correction for absorption is semi-empirical (crystal modeled either as an ellipsoid, or as a plate, with rejection of data within 3° of the primary X-ray beam).
† $R1 = [\Sigma||F_o| - |F_c||] / \Sigma|F_o| \times 100$
‡ $wR_2 = [\Sigma[w(F_o^2 - F_c^2)^2] / \Sigma[w(F_o^2)^2]]^{0.5} \times 100$, $w = 1/(\sigma^2(F_o^2) + (a \cdot P)^2$, and $P = 1/3 \max(0, F_o^2) + 2/3 F_c^2$.

TABLE 4. ATOM COORDINATES FOR URANOSPATHITE

RC3982	x	y	z	U_{eq}	Wyckoff position
U(1)	0.2214(1)	0.2543(1)	0.2477(3)	0.014(1)	4c
P(1)	0.2505(1)	0.7546(4)	0.2465(11)	0.016(1)	4c
Al(1)*	0	½	0.9578(7)	0.017(1)	2b
O(1)	0.2806(1)	0.2563(10)	0.2356(18)	0.020(1)	4c
O(2)	0.1621(2)	0.2547(11)	0.2595(18)	0.019(1)	4c
O(3)	0.2194(3)	0.5794(8)	0.2736(18)	0.016(2)	4c
O(4)	0.2776(3)	0.7790(9)	0.4233(11)	0.011(2)	4c
O(5)	0.2199(3)	0.9266(9)	0.2179(17)	0.021(2)	4c
O(6)	0.2839(3)	0.7241(11)	0.0780(13)	0.020(2)	4c
O(7)	−0.0267(3)	0.3410(10)	0.7789(11)	0.038(2)	4c
O(8)	−0.0189(3)	0.3281(11)	0.1446(11)	0.036(2)	4c
O(9)	0.0544(3)	0.3508(12)	0.9487(11)	0.042(2)	4c
O(10)	0.1376(4)	0.4784(15)	0.8421(15)	0.039(3)	4c
O(11)	0.1401(4)	0.0245(14)	0.6477(15)	0.035(3)	4c
O(12)	0.1409(4)	0.6660(15)	0.4836(16)	0.039(3)	4c
O(13)	0.1416(3)	0.8489(14)	0.0104(14)	0.032(3)	4c
O(14)	0.0617(3)	0.0000(11)	0.1109(12)	0.036(2)	4c
O(15)	0.0611(3)	0.5307(12)	0.4536(12)	0.038(2)	4c
O(16)	0.0657(3)	0.1452(12)	0.4750(12)	0.036(2)	4c
O(17)	0	0	0.6714(16)	0.032(3)	2a

U_{eq} is defined as one third of the trace of the orthogonalized U_{ij} tensor.
* Refined occupancy 86(1)%.

respectively. Observed and calculated structure-factors are available from the Depository of Unpublished Data, CISTI, National Research Council, Ottawa, Ontario K1A 0S2, Canada.

Bond-valence sums at the cation and anion sites of uranospathite and *AlUP* were calculated assuming full occupancy of all cation sites and using the parameters of Burns *et al.* (1997) for U, and those of Brown & Altermatt (1985) for P and Al. For uranospathite, the bond-valence sums at the U(1), P(1) and Al(1) sites

are 6.02, 4.97 and 3.14 valence units (*vu*) respectively, consistent with expected formal valences of U^{6+}, P^{5+} and Al^{3+}. The bond-valence sums for O(7) to O(17) range from 0 to 0.56 *vu*, consistent with their assignment as H_2O groups, whereas the bond-valence sums for O(1) to O(6) range from 1.69 to 2.05 *vu*. For *AlUP*, the bond-valence sums at the U(1), U(2), P(1), P(2), and Al(1) sites are 6.26, 6.00, 5.05, 4.88 and 2.99 *vu*, respectively, consistent with expected formal valences of U^{6+}, P^{5+} and Al^{3+}. The bond-valence sums for O(13) to O(28) range from 0 to 0.56 *vu*, consistent with their assignment as H_2O groups, whereas the bond-valence sums for O(1) to O(12) range from 1.60 to 2.06 *vu*.

TABLE 5. ATOM COORDINATES FOR $Al_{0.67}\square_{0.33}[(UO_2)(PO_4)]_2(H_2O)_{15.5}$

AlUP	x	y	z	U_{eq}
U(1)	0.2336(1)	0.5639(1)	0.3622(1)	0.016(1)
U(2)	-0.2328(1)	0.4367(1)	0.1379(1)	0.013(1)
P(1)	-0.2494(6)	0.4993(4)	0.3734(3)	0.020(1)
P(2)	0.2486(6)	0.5014(3)	0.1230(3)	0.014(1)
Al(1)*	-0.4863(14)	-0.0095(7)	0.2504(7)	0.041(2)
O(1)	-0.1931(16)	0.4336(8)	0.4745(8)	0.027(3)
O(2)	0.2100(13)	0.5721(7)	0.0228(7)	0.015(2)
O(3)	0.0981(14)	0.4250(8)	0.1550(8)	0.026(3)
O(4)	-0.4380(18)	0.5681(9)	0.3736(9)	0.034(4)
O(5)	0.2680(14)	0.5606(8)	0.2010(7)	0.023(2)
O(6)	0.4450(12)	0.4339(7)	0.1218(6)	0.012(2)
O(7)	-0.2484(13)	0.4229(7)	0.3031(7)	0.017(2)
O(8)	-0.0899(13)	0.5623(7)	0.3506(7)	0.018(2)
O(9)	0.2770(16)	0.4306(6)	0.3863(8)	0.027(3)
O(10)	-0.2632(15)	0.5706(7)	0.1106(8)	0.024(3)
O(11)	0.1978(16)	0.6940(6)	0.3420(8)	0.030(3)
O(12)	-0.1959(14)	0.3003(6)	0.1689(7)	0.021(2)
O(13)	0.4229(13)	0.2505(7)	0.0599(6)	0.023(2)
O(14)	-0.0421(19)	0.7524(10)	0.0327(10)	0.046(4)
O(15)	0.0555(18)	0.2492(10)	0.4775(9)	0.044(4)
O(16)	-0.2250(30)	0.7328(14)	0.2242(13)	0.091(6)
O(17)	0.2196(13)	0.2456(7)	0.2936(7)	0.026(2)
O(18)	0.3976(19)	0.7529(10)	0.1197(9)	0.050(4)
O(19)	-0.4170(20)	0.2337(11)	0.3781(10)	0.053(4)
O(20)	-0.0233(17)	0.0837(9)	0.1049(9)	0.047(3)
O(21)	0.3870(30)	0.2610(14)	0.5572(13)	0.091(6)
O(22A) †	-0.0050(30)	0.0521(15)	0.5108(15)	0.037(5)
O(23) ‡	-0.3520(20)	0.0843(13)	0.1698(12)	0.096(2)
O(24) ‡	-0.5150(30)	-0.0511(13)	0.1266(11)	0.096(2)
O(25) ‡	-0.2390(30)	-0.0868(13)	0.2475(13)	0.096(2)
O(26) ‡	-0.4040(30)	0.0498(13)	0.3576(13)	0.096(2)
O(27) ‡	-0.5870(30)	-0.1166(13)	0.3278(13)	0.096(2)
O(28) ‡	-0.7280(30)	0.0727(14)	0.2280(13)	0.096(2)

U_{eq} is defined as one third of the trace of the orthogonalized U_{ij} tensor.
* Occupancy constrained to be ⅔.
† Half-occupied, atom separated from symmetry-equivalent by 1.51(4) Å.
‡ Displacement parameters constrained to be equal.

TABLE 6. ANISOTROPIC DISPLACEMENT PARAMETERS ($Å^2$) FOR URANOSPATHITE

	U_{11}	U_{22}	U_{33}	U_{23}	U_{13}	U_{12}
U(1)	0.017(1)	0.012(1)	0.012(1)	-0.001(1)	-0.002(1)	0.000(1)
P(1)	0.022(1)	0.013(1)	0.012(1)	0.002(2)	-0.010(3)	-0.004(1)
Al(1)	0.019(3)	0.015(2)	0.018(3)	0	0	-0.001(2)

The anisotropic displacement parameter exponent takes the form:
$-2\pi^2 [h^2\mathbf{a}^{*2}U_{11} + ... + 2hk\mathbf{a}^*\mathbf{b}^* U_{12}]$.

TABLE 7. ANISOTROPIC DISPLACEMENT PARAMETERS ($Å^2$) FOR $Al_{0.67}\square_{0.33}[(UO_2)(PO_4)]_2(H_2O)_{15.5}$

	U_{11}	U_{22}	U_{33}	U_{23}	U_{13}	U_{12}
U(1)	0.012(1)	0.028(1)	0.009(1)	-0.007(1)	0.004(1)	-0.004(1)
U(2)	0.010(1)	0.016(1)	0.0011(1)	-0.002(1)	-0.001(1)	-0.001(1)
P(1)	0.012(2)	0.042(3)	0.008(2)	-0.009(2)	0.001(2)	-0.005(2)
P(2)	0.012(2)	0.016(2)	0.012(2)	-0.002(2)	0.002(2)	-0.001(2)

The anisotropic displacement parameter exponent takes the form:
$-2\pi^2 [h^2\mathbf{a}^{*2}U_{11} + ... + 2hk\mathbf{a}^*\mathbf{b}^* U_{12}]$.

TABLE 8. SELECTED INTERATOMIC DISTANCES (Å) AND ANGLES (°) FOR URANOSPATHITE

U(1)-O(1)	1.779(4)	O(11)-O(16)	2.680(13)
U(1)-O(2)	1.783(4)	O(11)-O(6)	2.720(13)
U(1)-O(3)	2.287(6)	O(11)-O(12)	2.767(14)
U(1)-O(4)	2.294(9)	O(11)-O(13)	2.838(13)
U(1)-O(5)	2.307(7)		
U(1)-O(6)	2.343(10)	O(12)-O(15)	2.585(13)
<U(1)-O$_{up}$>	1.78	O(12)-O(11)	2.767(14)
<U(1)-O$_{eq}$>	2.31	O(12)-O(3)	2.848(14)
O(1)-U(1)-O(2)	179.4(3)	O(12)-O(10)	2.850(15)
P(1)-O(4)	1.498(10)	O(13)-O(14)	2.716(13)
P(1)-O(5)	1.528(7)	O(13)-O(5)	2.822(14)
P(1)-O(3)	1.555(7)	O(13)-O(11)	2.838(13)
P(1)-O(6)	1.570(12)	O(13)-O(10)	2.857(13)
<P(1)-O>	1.54		
		O(14)-O(8)	2.645(11)
Al(1)-O(7)	1.864(8) × 2	O(14)-O(13)	2.716(13)
Al(1)-O(8)	1.872(8) × 2	O(14)-O(9)	2.721(11)
Al(1)-O(9)	1.940(9) × 2	O(14)-O(16)	2.764(12)
<Al(1)-O>	1.89		
		O(15)-O(12)	2.585(13)
O(7)-O(17)	2.633(8)	O(15)-O(7)	2.670(12)
O(7)-O(15)	2.670(12)	O(15)-O(8)	2.708(11)
		O(15)-O(16)	2.710(11)
O(8)-O(14)	2.645(11)		
O(8)-O(15)	2.708(11)	O(16)-O(17)	2.616(10)
		O(16)-O(11)	2.680(13)
O(9)-O(14)	2.721(11)	O(16)-O(15)	2.710(11)
O(9)-O(10)	2.756(15)	O(16)-O(14)	2.764(12)
O(10)-O(9)	2.756(15)	O(17)-O(16)	2.616(10) × 2
O(10)-O(12)	2.850(15)	O(17)-O(7)	2.633(8) × 2
O(10)-O(13)	2.857(13)		
O(10)-O(4)	2.962(14)		

The site occupancy (Hawthorne *et al.* 1995) of Al(1) in uranospathite refined to 86(1)%, giving rise to the empirical formula: $Al_{0.86}\square_{0.14}[(UO_2)(PO_4)]_2(H_2O)_{21}$, which is not electroneutral (net positive charge of 0.58 electrons per formula unit). Because of this discrepancy, the possibility of the presence of fluorine was tested and confirmed by qualitative WDS on similar samples (Fig. 3). The small difference in X-ray scattering efficiency between O and F prevents accurate determination of the location of a low proportion of F in the structure model. We believe that F substitutes for part of the H_2O coordinating Al in the structure; ideal Al–F bond lengths differ from Al–O bond lengths by less than 0.1 Å (Shannon 1976). The presence of fluorine leads to the empirical formula $Al_{0.86}\square_{0.14}[(UO_2)(PO_4)]_2$ $(H_2O)_{20.42}F_{0.58}$, which can be generalized (assuming varying Al and F contents and no anion vacancies) to the hypothetical formula $Al_{1-x}\square_x[(UO_2)(PO_4)]_2$ $(H_2O)_{20+3x}F_{1-3x}$, $0 < x < 0.33$.

The small amount of uranospathite available for investigation precluded the use of bulk methods to determine independently the amount of Al and F present, and the beam-sensitive nature of this material prevented quantitative analysis with the use of an electron microprobe. We are aware that as Nature abhors a vacuum [Rabelais, F. (1490–1553) wrote, in Gargantua and Pantagruel: "*Natura abhorret vacuum*"], so also do mineralogists abhor a vacancy. We have no independent measure as to the accuracy of the site-scattering refinement of the Al position, only the refined value and the associated estimate of uncertainty derived from the least-squares covariance matrix: 86(1)%. However, although the estimated standard deviations of structural parameters are routinely underestimated (Taylor & Kennard 1986, Schwarzenbach 1991), and are less precise in a heavy-atom structure, the Al position is still underoccupied (within 10σ estimated uncertainty). Thus, it is likely that the Al site is at least partially vacant.

The site occupancy of Al(1) in *AlUP* refined to partial occupancy, but is highly correlated to the magnitude of its equivalent isotropic displacement parameter.
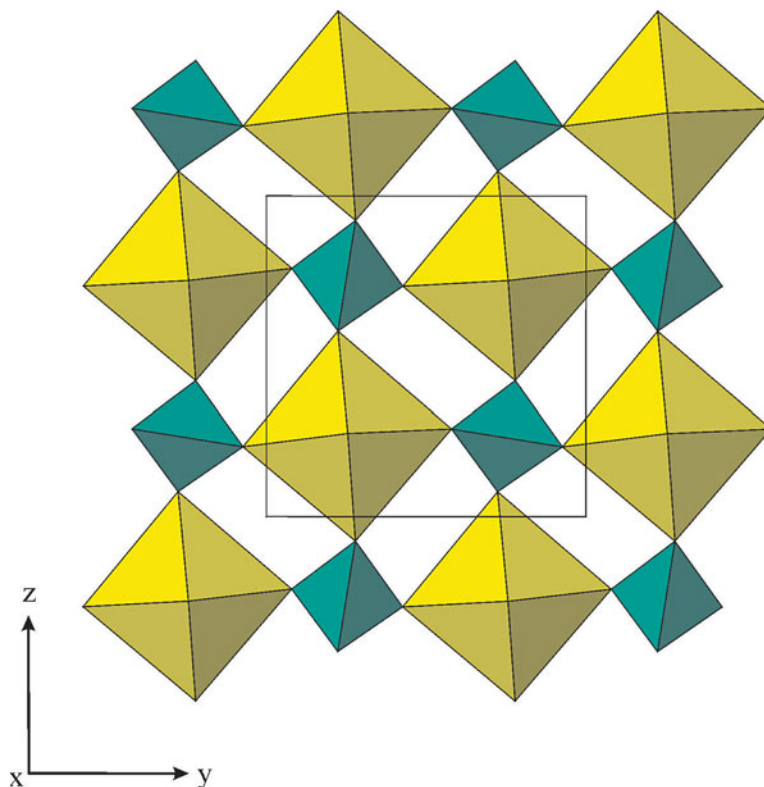

FIG. 4.   The autunite-type uranyl phosphate sheet in uranospathite, projected along [100]. The uranyl square bipyramids are yellow, and the phosphate tetrahedra are green.
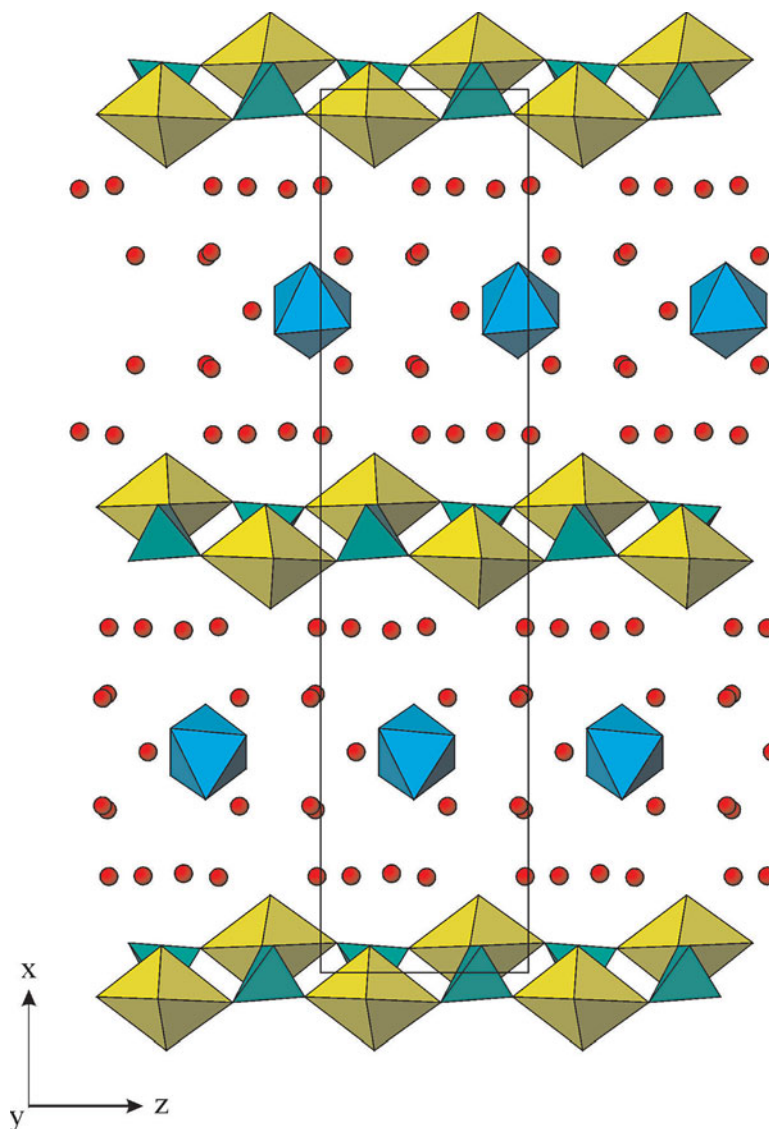
FIG. 5.   The structure of uranospathite, projected along [010]. Uranyl polyhedra are yellow, phosphate tetrahedra are green, aluminum-centered octahedra are blue, and H_2O groups are shown as red spheres.

To maintain electroneutrality, the occupancy of this site was fixed at ⅔, which yielded a reasonable displacement parameter (Table 5).

DESCRIPTION OF THE STRUCTURES

Both uranospathite and *AlUP*, like other members of the autunite and meta-autunite groups (Burns 1999), contain the well-known corrugated autunite-type sheet formed by the sharing of vertices between uranyl square bipyramids and phosphate tetrahedra (Fig. 4), with composition $[(UO_2)(PO_4)]^-$, which was originally described by Beintema (1938). The relative orientations of the uranyl phosphate sheets in uranospathite are similar to those of autunite-group minerals; every second sheet is offset by [0, ½, ½], which creates large interlayer cavities (Beintema 1938); the uranyl phosphate sheets of *AlUP* are aligned in a similar fashion.

The interlayer between the uranyl phosphate sheets of uranospathite is complex and contains one Al position, and eleven symmetrically independent H_2O groups. The Al(1) position is in distorted octahedral coordination by the O(7), O(8) and O(9) H_2O groups (Table 8, Fig. 5). Eight additional H_2O positions, O(10) to O(17), occur in the interlayer and are held in the structure only by hydrogen bonding. A network of hydrogen bonds is proposed in which each of these eight H_2O group has fourfold links, with D...A interatomic distances in the range 2.5–3.0 Å (Table 8, Fig. 6). The arrangement of the interlayer H_2O groups leads to tilting of the Al octahedra, and prevents the structure from being centrosymmetric (Figs. 5, 6).

The H_2O groups in uranospathite can be divided conveniently into three categories: 1) those forming fourfold square planar sets, 2) those coordinating Al, and 3) those linking the previous two categories. Thus, in category 1), H-bonds link O(10), O(11), O(12) and O(13) into a square-planar set of H_2O groups, with further H-bonds extending to acceptors in the uranyl phosphate sheet, O(4), O(6), O(3) and O(5), respectively. The proposed H-bond acceptors in the uranyl phosphate sheets are the anions at the equatorial vertices of uranyl square bipyramids that are also shared with phosphate tetrahedra. Hydrogen bonds also extend from this square planar set to other H_2O groups in the interlayer, O(9), O(16), O(15), and O(14), respectively. In category 2), the H_2O groups that form the octahedron around Al(1), O(7), O(8), and O(9), are in three-fold coordination, each having two links by H-bonds to interlayer H_2O groups in addition to the bond to Al. Hydrogen bonds link O(7) with O(15) and O(17), O(8) with O(14) and O(15), and O(9) with O(14) and with the O(10) position of the square planar set of H_2O groups (Table 8, Fig. 6). In category 3), O(14), O(15), O(16), and O(17) are linked by H-bonds to the H_2O groups of the square planar set, the H_2O groups coordinating Al, and to each other (Table 8, Fig. 6).

Although the F content necessary for charge balance could not be located precisely in the structure of uranospathite, it is likely that it substitutes partially for the H_2O groups of O(7) or O(8) (or both) as these positions have the shortest Al–O interatomic distances (Table 8), and are thus most similar to the ideal Al–F bond length of ~1.83 Å (Shannon 1976). Maximum F occupancy (1 F atom per formula unit) corresponds to only half of one of these positions. In the hypothetical end-member case where H_2O is present instead of F, and the Al position is only ⅔ occupied, $Al_{0.67}\square_{0.33}[(UO_2)(PO_4)]_2(H_2O)_{21}$, it may be possible that the H-bond network is reconfigured, as the distances separating O(7), O(8) and O(9), 2.59 to 2.84 Å, are within the normal range for hydrogen bonds (Jeffrey 1997).

The interlayer of *AlUP* is similar to that of uranospathite; Al(1) occurs in distorted octahedral coordination by the O(23) – O(28) H_2O groups (Table 9, Fig. 7).

Ten additional H_2O positions, O(13) to O(22A), occur in the interlayer and are held in the structure only by hydrogen bonding. As in uranospathite, a H-bond network is proposed in which most of these H_2O groups have fourfold links, with D...A interatomic distances in the range 2.5–3.3 Å (Table 9, Fig. 7). The interlayer of *AlUP* is not as well behaved as that of uranospathite; for reasons of charge balance, the Al(1) position is ⅔ occupied, and the O(22A) position in *AlUP* is half-occupied, as the separation distance to its symmetry-equivalent is 1.51(4) Å. Like in uranospathite, square-planar sets of H_2O groups above and below the Al(1) position are linked by hydrogen bonds to acceptors in the uranyl phosphate sheet and to other H_2O groups in the interlayer, including those that coordinate aluminum (Fig. 7).

DISCUSSION

Comparison with previous work

The structure of uranospathite is orthorhombic, pseudotetragonal, in agreement with its biaxial optical properties (Walenta 1978) and the conclusions of Hallimond (1915). The chemical formula derived from the structure refinement, $Al_{0.86}\square_{0.14}[(UO_2)(PO_4)]_2$ $(H_2O)_{20.42}F_{0.58}$, differs from that of Walenta (1978), $(HAl)_{0.5}[(UO_2)(PO_4)]_2(H_2O)_{20}$, in the somewhat elevated content of Al, in the presence of F, and in the absence of H_3O^+. The Al contents of uranospathite and arsenuranospathite were determined by Walenta (1978) on the basis of results of semiquantitative electron-microprobe analyses of partially dehydrated material. In view of the beam-sensitive nature of these minerals (Fig. 1), inferior agreement between the electron-microprobe results and the structure model for the interlayer cation is not unexpected.

Although the structure of arsenuranospathite was not determined in this work, it is presumed to be isostructural with uranospathite because of the similarity of their cell dimensions (Walenta 1978), and the general isotypism of uranyl phosphates and uranyl arsenates of the autunite and meta-autunite groups, *e.g.*, torbernite and zeunerite, metatorbernite and metazeunerite (Locock & Burns 2003a).

The structure of *AlUP*, $Al_{0.67}\square_{0.33}[(UO_2)(PO_4)]_2$ $(H_2O)_{15.5}$, probably corresponds to the synthetic aluminum uranyl phosphate hexakaidecahydrate of Walenta (1978), $(HAl)_{0.5}[(UO_2)(PO_4)]_2(H_2O)_{16}$, although the latter compound was reported to have a tetragonal unit-cell, *a* 6.97 Å, *c* 26.43 Å, D_{calc} 2.67 g/mL. The basal *d*-value, d_{010}, of *AlUP*, calculated using the program XPOW (Downs *et al.* 1993), is 13.29 Å, similar to the 13.15 Å reported by Walenta (1978), and their stoichiometries and calculated densities are similar.

Uranospathite, $Al_{1-x}\square_x[(UO_2)(PO_4)]_2(H_2O)_{20+3x}$ F_{1-3x}, $0 < x < 0.33$, is the "Dagwood sandwich" of the autunite group, with a large interlayer spacing, d_{200} of 15.01 Å (Fig. 5). In contrast, the interlayer spacings of the known structures of autunite-group uranyl phosphates are generally around 10 Å: torbernite, $Cu[(UO_2)(PO_4)]_2(H_2O)_{12}$, $d_{002} = 10.40$ Å; autunite, $Ca[(UO_2)(PO_4)]_2(H_2O)_{11}$, $d_{020} = 10.35$ Å; and saléeite, $Mg[(UO_2)(PO_4)]_2(H_2O)_{10}$, $d_{020} = 9.97$ Å (Locock & Burns 2003a, b, Miller & Taylor 1986). The larger interlayer spacings in uranospathite and *AlUP* result from their high degrees of hydration in comparison to that in those structures.

The presence of up to four distinct hydration states (21 H_2O *pfu* = uranospathite, 15.5 = *AlUP*, 10, and 8 = sabugalite?) in aluminum uranyl phosphates with the autunite-type sheet (Walenta 1978) calls into question the traditional division of the autunite and meta-autunite groups. Conventionally, autunite-group uranyl phosphates have cell dimensions that can approximate a tetragonal unit-cell: $a = 7$ Å, $c = 20$ Å, and have 10–12 H_2O groups per formula unit on the basis of $[(UO_2)(PO_4)]_2^{2-}$, whereas meta-autunite-group uranyl phosphates approximate a smaller cell: $a = 7$ Å, c in the range 17–18 Å, and have 6–8 H_2O groups per formula unit on the basis of $[(UO_2)(PO_4)]_2^{2-}$. In addition, the orientations of the uranyl phosphate sheets differ between the groups. In meta-autunite-group compounds, corresponding points in adjacent sheets lie directly above each other, whereas in autunite-group compounds, every second sheet is offset (by [½, ½, 0], assuming that the sheets are perpendicular to [001]), to provide fewer but larger interlayer cavities (Beintema 1938). The tacit assumption has been that only two hydration states are present for a given interlayer cation. However, both the Al- and Ba-uranyl phosphate hydrate systems show more than two hydration states (Walenta 1965, 1978), and thus consideration should be given to combining the current autunite and meta-autunite groups into a single comprehensive group, in which membership is based only on the presence of the autunite-type sheet, not the relative orientations of these sheets and various hydration states.

TABLE 9. SELECTED INTERATOMIC DISTANCES (Å) AND ANGLES (°)
FOR $Al_{0.67}\square_{0.33}[(UO_2)(PO_4)]_2(H_2O)_{15.5}$

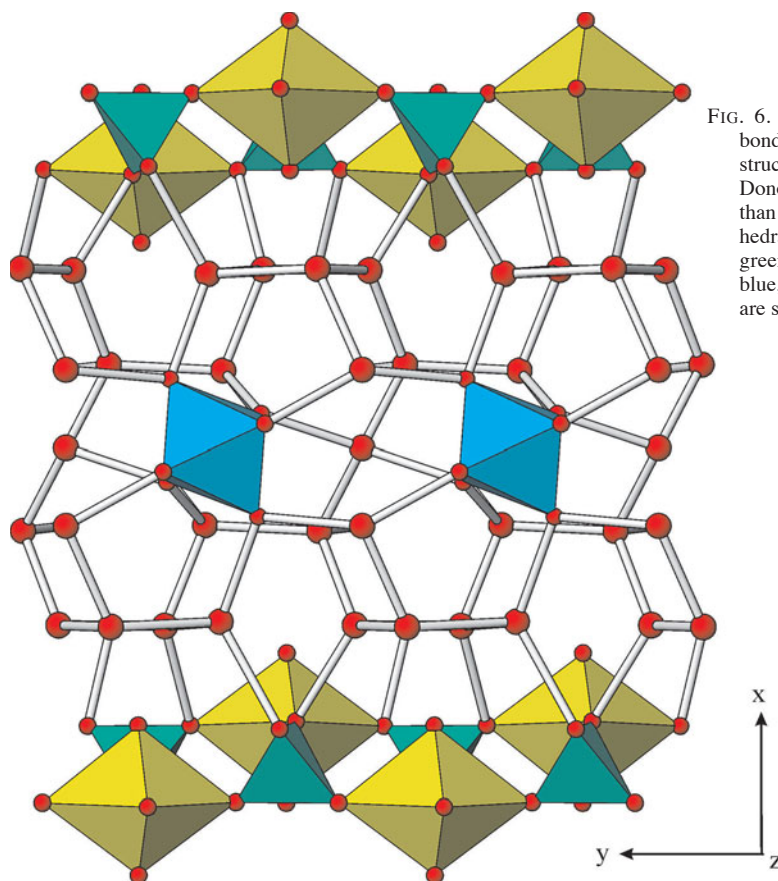|					
U(1)-O(11)	1.732(8)	Al(1)-O(27)	1.86(2)	O(18)-O(13)	2.814(16)
U(1)-O(9)	1.772(7)	Al(1)-O(23)	1.886(15)	O(18)-O(24)	2.86(2)
U(1)-O(8)	2.275(9)	Al(1)-O(28)	1.888(19)	O(18)-O(16)	2.98(2)
U(1)-O(5)	2.281(10)	Al(1)-O(25)	1.904(19)	O(18)-O(5)	2.922(17)
U(1)-O(1)	2.314(11)	Al(1)-O(24)	1.953(14)		
U(1)-O(4)	2.316(13)	Al(1)-O(26)	1.971(19)	O(19)-O(26)	2.59(2)
<U(1)-O$_{up}$>	1.75	<Al(1)-O>	1.91	O(19)-O(17)	2.785(17)
<U(1)-O$_{eq}$>	2.30			O(19)-O(21)	2.92(2)
O(11)-U(1)-O(9)	177.8(5)	O(13)-O(23)	2.77(2)	O(19)-O(7)	2.997(17)
		O(13)-O(18)	2.814(16)		
U(2)-O(10)	1.781(9)	O(13)-O(6)	2.844(12)	O(20)-O(23)	2.47(2)
U(2)-O(12)	1.814(9)	O(13)-O(14)	2.981(16)	O(20)-O(28)	2.67(2)
U(2)-O(6)	2.275(9)			O(20)-O(14)	2.744(18)
U(2)-O(2)	2.285(9)			O(20)-O(25)	3.29(2)
U(2)-O(7)	2.290(9)	O(14)-O(20)	2.744(18)		
U(2)-O(3)	2.310(10)	O(14)-O(2)	2.854(16)		
<U(2)-O$_{up}$>	1.80	O(14)-O(16)	2.95(2)	O(21)-O(27)	2.54(3)
<U(2)-O$_{eq}$>	2.29	O(14)-O(13)	2.981(16)	O(21)-O(15)	2.62(2)
O(10)-U(2)-O(12)	178.0(5)			O(21)-O(4)	2.78(2)
		O(15)-O(21)	2.62(2)	O(21)-O(19)	2.92(2)
P(1)-O(8)	1.502(9)	O(15)-O(22A)	2.74(2)		
P(1)-O(4)	1.511(13)	O(15)-O(17)	2.824(15)	O(22A)-O(15)	2.74(2)
P(1)-O(1)	1.539(11)	O(15)-O(1)	2.853(17)		
P(1)-O(7)	1.575(10)			O(23)-O(13)	2.77(2)
<P(1)-O>	1.53	O(16)-O(25)	2.55(3)	O(23)-O(20)	2.47(2)
		O(16)-O(8)	2.69(2)		
P(2)-O(5)	1.503(10)	O(16)-O(18)	2.98(2)	O(24)-O(18)	2.86(2)
P(2)-O(2)	1.540(10)	O(16)-O(10)	3.03(2)		
P(2)-O(6)	1.547(9)			O(25)-O(16)	2.55(3)
P(2)-O(3)	1.590(10)	O(17)-O(28)	2.69(2)		
<P(2)-O>	1.55	O(17)-O(19)	2.785(17)	O(26)-O(19)	2.59(2)
		O(17)-O(15)	2.824(15)		
		O(17)-O(3)	2.839(15)	O(27)-O(21)	2.54(3)
				O(28)-O(20)	2.67(2)
				O(28)-O(17)	2.69(2)

FIG. 6.   A possible scheme of hydrogen bonding in a portion of the uranospathite structure is shown, projected along [001]. Donor–acceptor (O...O) distances of less than 3.0 Å are shown as rods. Uranyl polyhedra are yellow, phosphate tetrahedra are green, aluminum-centered octahedra are blue, and both O atoms and H_2O groups are shown as red spheres.
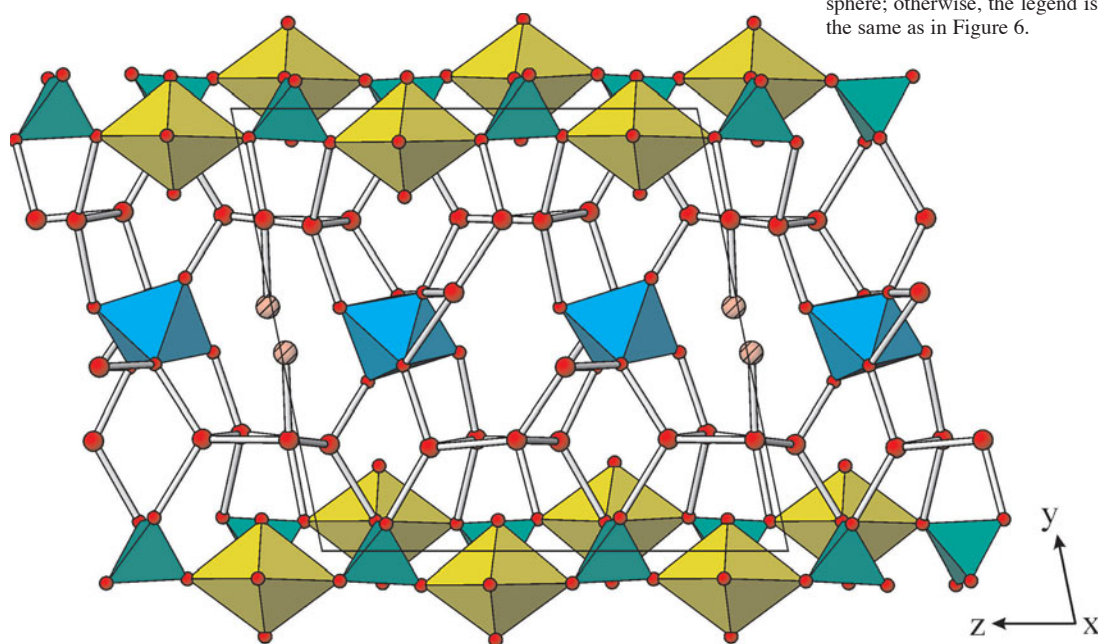
FIG. 7.   The structure of *AlUP*, $Al_{0.67}\square_{0.33}[(UO_2)(PO_4)]_2(H_2O)_{15.5}$, projected along [100]. A possible scheme of hydrogen bonding is shown, with donor–acceptor (O...O) distances of less than 3.3 Å. The O(22A) position is shown as a striped pale red sphere; otherwise, the legend is the same as in Figure 6.

*Other aluminum uranyl phosphates
of the autunite and meta-autunite groups*

Threadgoldite, $Al[(UO_2)(PO_4)]_2(OH)(H_2O)_8$, is the only other aluminum uranyl phosphate mineral of the autunite and meta-autunite groups that has a known structure (Khosrawan-Sazedj 1982, Piret *et al.* 1979a, Deliens *et al.* 1979a). The most significant difference between uranospathite and threadgoldite lies in the coordination environment of aluminum, which in threadgoldite occurs in the interlayer as a dimer of edge-sharing distorted octahedra: $\{Al_2(OH)_2(H_2O)_8\}$; there are four additional H_2O positions held in this structure only by hydrogen-bonding. In contrast, aluminum occurs as an isolated $Al(H_2O)_6$ octahedron in uranospathite (ignoring the minor F content), and hydroxyl is not present.

The structure of sabugalite, $(HAl)_{0.5}[(UO_2)(PO_4)]_2$ $(H_2O)_{8-10?}$, has not yet been determined, and thus its true symmetry and chemical formula remain uncertain. If sabugalite does correspond to a lower hydrate of uranospathite, it can be expected that the Al position(s) may be partially occupied and that in natural systems, F may be present to play the same charge-balancing role as in uranospathite and arsenuranospathite.

REFERENCES

ANTHONY, J.W., BIDEAUX, R.A., BLADH, K.W. & NICHOLS, M.C. (2000): *Handbook of Mineralogy.* **IV**. *Arsenates, Phosphates, Vanadates*. Mineral Data Publishing, Tucson, Arizona.

AREND, H. & CONNELLY, J.J. (1982): Tetramethoxysilane as gel forming agent in crystal growth. *J. Crystal Growth* **56**, 642-644.

BEINTEMA, J. (1938): On the composition and crystallography of autunite and the meta-autunites. *Recl. Trav. Chim. Pays-Bas* **57**, 155-175.

BROWN, I.D. & ALTERMATT, D. (1985): Bond-valence parameters obtained from a systematic analysis of the inorganic crystal structure database. *Acta Crystallogr.* **B41**, 244-247.

BRUKER–AXS (1998): *SAINT, V 5.01 program for reduction of data collected on Bruker AXS CCD area detector systems*. Bruker Analytical X-ray Systems, Madison, Wisconsin.

BÜLTEMANN, W.D. (1979): Die Uranlagerstätte "Krunkelbach" bei Menzenschwand, Hochschwarzw. und ihr geologisch-lagestättenkundlicher Rahmen. *Z. Deutsch. Geol. Ges.* **130**, 597-618.

BURNS, P.C. (1999): The crystal chemistry of uranium. *In* Uranium: Mineralogy, Geochemistry and the Environment (P.C. Burns & R. Finch, eds.). *Rev. Mineral.* **38**, 23-90.

_____, EWING, R.C. & HAWTHORNE, F.C. (1997): The crystal chemistry of hexavalent uranium: polyhedron geometries, bond-valence parameters, and polymerization of polyhedra. *Can. Mineral.* **35**, 1551-1570.

ČEJKA, J. (1999): Infrared spectroscopy and thermal analysis of the uranyl minerals. *In* Uranium: Mineralogy, Geochemistry and the Environment (P.C. Burns & R. Finch, eds.). *Rev. Mineral.* **38**, 521-622.

CHERVET, J. & BRANCHE, G. (1955): Contribution à l'études des minéraux secondaires d'uranium français. *Sci. de la Terre* **3**, 1-186.

DELIENS, M., HENRIOT, O., MATHIS, V. & CAUBEL, A. (1991): *Minéraux des gisements d'uranium du Lodévois*. Association Française de Microminéralogie, 61 p.

_____ & PIRET, P. (1979a): Uranyl and aluminum phosphates from Kobokobo [Kivu, Zaire]. IV. Threadgoldite, $Al(UO_2)_2(PO_4)_2(OH)\bullet8H_2O$. *Bull. Minéral.* **102**, 338-341.

_____ & _____ (1979b): Ranunculite, $AlH(UO_2)(PO_4)$ $(OH)_3\bullet4H_2O$, a new mineral. *Mineral. Mag.* **43**, 321-323.

_____ & _____ (1981): Les phosphates d'uranyle et d'aluminium de Kobokobo. V. La mundite, nouveau minéral. *Bull. Minéral.* **104**, 669-671.

_____ & _____ (1982): Les phosphates d'uranyle et d'aluminium de Kobokobo. VI. La triangulite, $Al_3(UO_2.PO_4)_4(OH)_5\bullet5H_2O$, nouveau minéral. *Bull. Minéral.* **105**, 611-614.

_____ & _____ (1984): La kamitugaïte, Pb Al$(UO_2)_5[$ $(P,As)O_4]_2(OH)_9\bullet9,5\ H_2O$, nouveau minéral de Kobokobo, Kivu, Zaïre. *Bull. Minéral.* **107**, 15-19.

_____ & _____ (1985a): Les phosphates d'uranyle et d'aluminium de Kokobo. VII. La moreauïte. *Bull. Minéral.* **108**, 9-13.

_____ &_____ (1985b): Les phosphates d'uranyle et d'aluminium de Kokobo. VIII. La furongite. *Ann. Soc. Geol. Belg.* **108**, 365-368.

DOWNS, R.T., BARTELMEHS, K.L., GIBBS, G.V. & BOISEN, JR., M.B. (1993): Interactive software for calculating and displaying X-ray or neutron powder diffractometer patterns of crystalline materials. *Am. Mineral.* **78**, 1104-1107.

EMBREY, P.G. & SYMES, R.F. (1987): *Minerals of Cornwall and Devon*. British Museum (Natural History), London, U.K.

FINCH, R. & MURAKAMI, T. (1999): Systematics and paragenesis of uranium minerals. *In* Uranium: Mineralogy, Geochemistry and the Environment (P.C. Burns & R. Finch, eds.). *Rev. Mineral.* **38**, 91-180.

FRONDEL, C. (1951): Studies of uranium minerals. VIII. Sabugalite, an aluminum-autunite. *Am. Mineral.* **36**, 671-679.

_____ (1954): Bassetite and uranospathite. *Mineral. Mag.* **30**, 343-353.

_____ (1958): Systematic mineralogy of uranium and thorium. *U.S. Geol. Surv., Bull.* **1064**.

HALLIMOND, A. F. (1915): On bassetite and uranospathite, new species hitherto classed as autunite. *Mineral. Mag.* **17**, 221-236.

_____ (1954): Note by A. F. Hallimond (February 1954). *Mineral. Mag.* **30**, 353.

HAWTHORNE, F.C., UNGARETTI, L. & OBERTI, R. (1995): Site populations in minerals: terminology and presentation of results of crystal-structure refinement. *Can. Mineral.* **33**, 907-911.

HENISCH, H.K. (1988): *Crystals in Gels and Liesegang Rings*. Cambridge University Press, New York, N.Y.

JEFFREY, G.A. (1997): *An Introduction to Hydrogen Bonding*. Oxford University Press, Oxford, U.K.

KHOSRAWAN-SAZEDJ, F. (1982): On the space group of threadgoldite. *Tschermaks Mineral. Petrogr. Mitt.* **30**, 111-115.

LE PAGE, Y. (1987): Computer derivation of the symmetry elements implied in a structure description. *J. Appl. Crystallogr.* **20**, 264-269.

LOCOCK, A.J. & BURNS, P.C. (2003a): Crystal structures and synthesis of the copper-dominant members of the autunite and meta-autunite groups: torbernite, zeunerite, metatorbernite and metazeunerite. *Can. Mineral.* **41**, 489-502.

_____ & _____ (2003b): The crystal structure of synthetic autunite, Ca[(UO$_2$)(PO$_4$)]$_2$(H$_2$O)$_{11}$. *Am. Mineral.* **88**, 240-244.

MANDARINO, J.A. & BACK, M.E. (2004): *Fleischer's Glossary of Mineral Species 2004*. The Mineralogical Record Inc., Tucson, Arizona.

MANGHI, E. & POLLA, G. (1983): Hydrogen uranyl arsenate hydrate single crystals: H$_2$(UO$_2$)$_2$(AsO$_4$)$_2$•8H$_2$O; gel growth and characterization. *J. Crystal Growth* **61**, 606-614.

MARSH, R.E. (1995) Some thoughts on choosing the correct space group. *Acta Crystallogr.* **B51**, 897-907.

MILLER, S.A. & TAYLOR, J.C. (1986): The crystal structure of saleeite, Mg[UO$_2$PO$_4$]$_2$•10H$_2$O. *Z. Kristallogr.* **177**, 247-253.

OTTOLINI, L., CÁMARA, F. & BIGI, S. (2000): An investigation of matrix effects in the analysis of fluorine in humite-group minerals by EMPA, SIMS and SREF. *Am. Mineral.* **85**, 89-102.

PERRINO, C.T. & LEMASTER, C.B. (1984): Preparation of HUO$_2$PO$_4$•4H$_2$O single crystals from gel. *J. Crystal Growth* **69**, 639-640.

PIRET, P. & DECLERCQ, J.-P. (1983): Structure cristalline de l'upalite Al[(UO$_2$)$_3$O(OH)(PO$_4$)$_2$]•7H$_2$O. Un exemple de macle mimétique. *Bull. Minéral.* **106**, 383-389.

_____, _____ & WAUTERS-STOOP, D. (1979a): Structure of threadgoldite. *Acta Crystallogr.* **B35**, 3017-3020.

_____ & DELIENS, M. (1987): Les phosphates d'uranyle et d'aluminium de Kokobo. IX. L'althupite AlTh(UO$_2$)[(UO$_2$)$_3$O(OH)(PO$_4$)$_2$]$_2$(OH)$_3$•15H$_2$O, nouveau minéral; propriétés et structure cristalline. *Bull. Minéral.* **110**, 65-72.

_____, PIRET-MEUNIER, J. & DECLERCQ, J.-P. (1979b): Structure of phuralumite. *Acta Crystallogr.* **B35**, 1880-1882.

RAUDSEPP, M. (1995): Recent advances in the electron-probe micro-analysis of minerals for the light elements. *Can. Mineral.* **33**, 203-218.

REED, S.J.B. (1993): *Electron Microprobe Analysis* (2nd ed.). Cambridge University Press, Cambridge, U.K. (275-291).

ROBERT, M.C. & LEFAUCHEUX, F. (1988): Crystal growth in gels: principle and applications. *J. Crystal Growth* **90**, 358-367.

SARIC, V. (1978): Leziste urana Zletovska reka. *Rad. Inst. Geol.-Rud. Istraz. Ispit. Nukl. Drugih Miner. Sirovina* **12**, 45-53 (in Serbo-Croatian).

SCHWARZENBACH, D. (1991): Statistical descriptors. *In* Crystallographic Computing. 5. From Chemistry to Biology (D. Moras, A.D. Podjarny & J.C. Thierry, eds.). Oxford University Press, Oxford, U.K. (69-78).

SHANNON, R.D. (1976): Revised effective ionic radii and systematic studies of interatomic distances in halides and chalcogenides. *Acta Crystallogr.* **A32**, 751-767.

SHELDRICK, G.M. (2000): *SHELXTL Version 6.10.* Bruker AXS, Madison, Wisconsin.

SPEK, A.L. (2003): Single-crystal structure validation with the program PLATON. *J. Appl. Crystallogr.* **36**, 7-13.

TAYLOR, R. & KENNARD, O. (1986) Accuracy of crystal structure error estimates. *Acta Crystallogr.* **B42**, 112-120.

VOCHTEN, R. & PELSMAEKERS, J. (1983): Synthesis, solubility, electrokinetic properties and refined crystallographic data of sabugalite. *Phys. Chem. Minerals* **9**, 23-29.

WALENTA, K. (1965): Die Uranglimmergruppe. *Chem. Erde* **24**, 254-278.

_____ (1978): Uranospathite and arsenuranospathite. *Mineral. Mag.* **42**, 117-128.

WILSON, A.J.C., ed. (1992): *International Tables for X-ray Crystallography, Vol. C.* Kluwer Academic Press, Boston, Massachussetts.

ZOLENSKY, M.E. (1983): *The Structures and Crystal Chemistry of the Autunite and Meta-Autunite Mineral Groups. Appendix 1. Gel Growth Experiments.* Ph.D. thesis, Pennsylvania State Univ., University Park, Pennsylvania.